iScience, Volume *26*

Supplemental information

LEAFY homeostasis is regulated via ubiquitin-dependent degradation and sequestration in cytoplasmic condensates

Ulla Dolde, Fernando Muzzopappa, Charlotte Delesalle, Julie Neveu, Fabian Erdel, and Grégory Vert

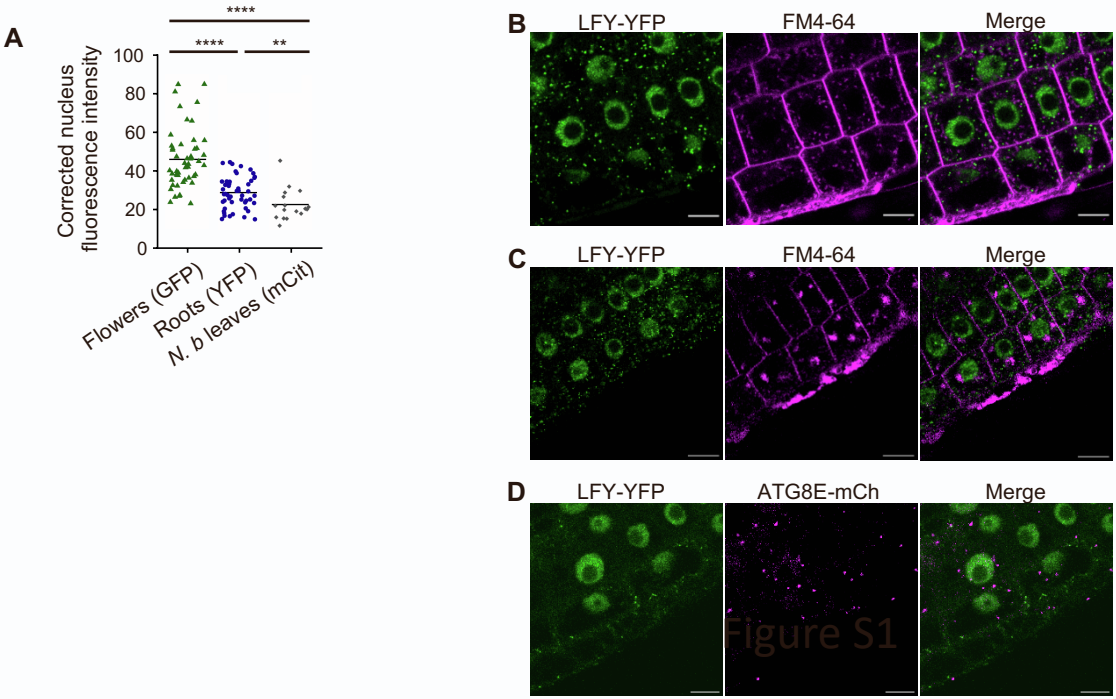

Supplemental Figure 1 LFY protein localizes to membraneless foci. Related to Figure 1. A, Fluorescence intensity analysis of LFY tagged with fluorescent proteins in flowers from *lfy-12*/LFY::LFY-GFP, in roots from 35S::LFY-YFP and in transiently-expressed 35S::LFY-mCit *N. benthamiana* leaves. Images were taken using similar settings and corrections for molecular brightness of fluorescent proteins applied. n = 18 of 3 independent experiments. Statistical significance was determined using a one-way ANOVA, B, Confocal microscopy images of root tips from 5-day-old 35S::LFY-YFP seedlings stained with FM4-64. Scale bar = 10 μm. C, Confocal microscopy images of root tips from 5-day-old 35S::LFY-YFP seedlings treated with BFA and stained with FM4-64. Scale bar = 10 μm. D, Confocal microscopy images of root tips from 5-day-old F1 plants resulting from a cross between 35S::LFY-YFP and 35S::ATG8E-mCh plants. Scale bar = 10 μm.

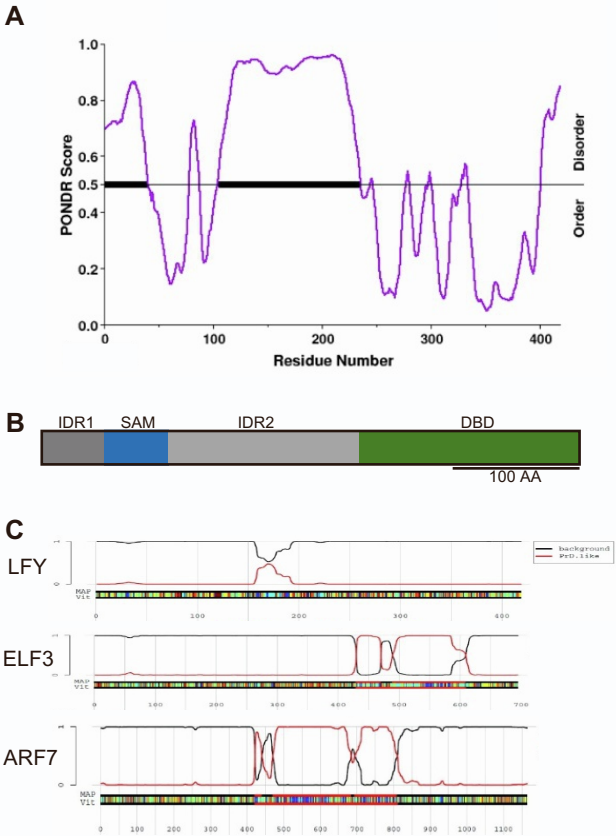

Supplemental Figure 2 LFY protein contains two IDRs. Related to Figure 2. A, Predictions of intrinsically disordered regions (IDRs) in LFY protein using the Predictor of Natural Disordered Regions (PONDR, http://www.pondr.com) algorithm. B, Representation of LFY depicting the IDRs (gray). LFY encodes a sterile alpha motif (SAM) and a DNA-binding domain (DBD). C, Predictions of prion-like domains (PLDs) in LFY protein using the Prion-Like Amino Acid Composition algorithm (PLAAC, http://plaac.wi.mit.edu)

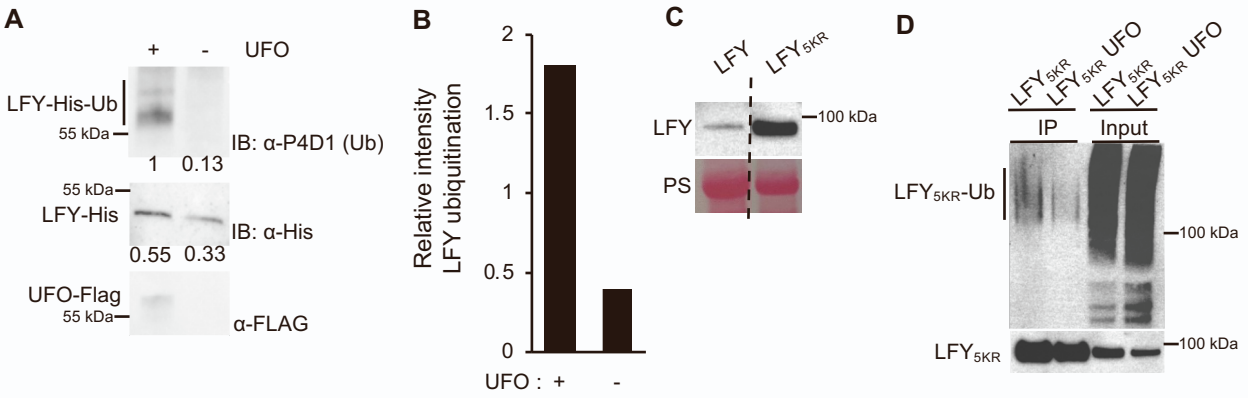

Supplemental Figure 3 Regulation of LFY levels by UFO-mediated ubiquitination and dependence on lysine residues in IDR. Related to Figure 4. A, *in vitro* ubiquitination assay of LFY-His recombinant protein in the presence or absence of UFO-FLAG. Ubiquitination is detected using anti-ubiquitin antibodies. B, Quantification of the ubiquitination signals shown in (A) relative to LFY-His levels. C, Total LFY protein levels in *N. benthamiana* leaves transiently expressing 35S::LFY-mCit or 35S::LFY_{5KR}-mCit. The blot has been cropped to remove unnecessary lanes. The LFY_{5KR} lane corresponds to Fig. 5K. Ponceau red staining (PS) serves as loading control. D, Ubiquitination profile of LFY_{5KR} protein in *N. benthamiana* leaves transiently expressing 35S::LFY_{5KR}-mCit or coexpressing 35S::LFY_{5KR}-mCit and 35S::UFO-mCh. LFY_{5KR}-mCit proteins were immunoprecipitated using anti-GFP antibodies and ubiquitination profile assessed using anti-ubiquitin antibodies (top panel). Immunodetection using anti-GFP antibodies serves as loading control (bottom panel). The input fractions for LFY-mCit levels were also used to evaluate the impact of UFO expression on LFY_{5KR}-mCit accumulation in Fig. 5K.

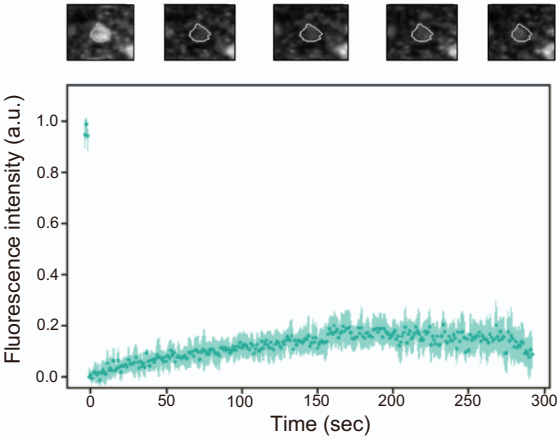

Supplemental Figure 4 LFY protein nucleocytoplasmic shuttling. Related to Figure 6. FRAP recovery profiles after photobleaching of whole nucleus from 5-day-old 35S::LFY-YFP roots. Top panel: representative nucleus during a FRAP experiment. Bottom panel: recovery profile of LFY-YFP fluorescence over time. n=8, independent experiments.

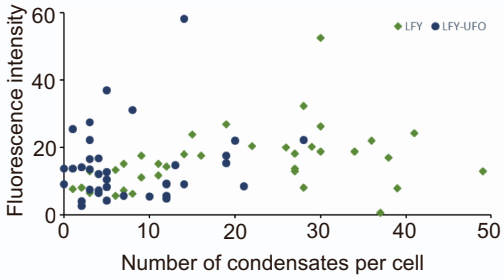

Supplemental Figure 5 Correlation between fluorescence intensity in the nucleus and number of condensates per cells from *N. benthamiana* leaves transiently expressing 35S::LFY-mCit or coexpressing 35S::LFY-mCit and 35S::UFO-mCh. Related to Figure 6.

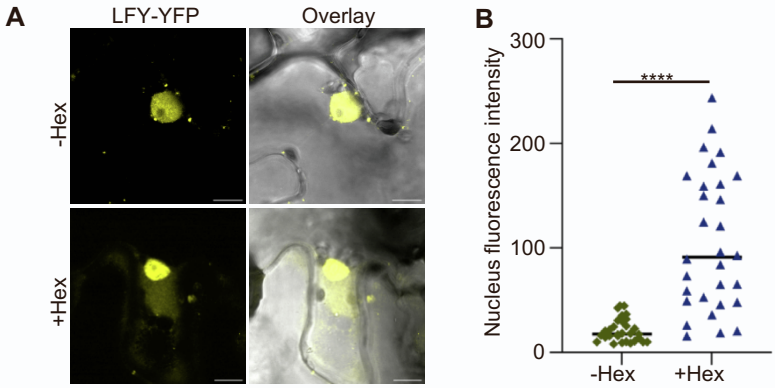

Supplemental Figure 6 LFY protein forms biomolecular condensates. Related to Figure 7. A, Transient expression of 35S::LFY-mCit in N. benthamiana leaves before and after treatment with 20% 1,6-hexanediol. Scale bar = 10 μm. B, Quantification of fluorescence intensity in the nucleus of N. benthamiana leaves transiently expressing 35S::LFY-YFP before and after treatment with 20% 1,6-hexanediol as shown in (A). n = 30 of 3 independent experiments. Statistical significance was determined using a two-tailed Student's t-test.

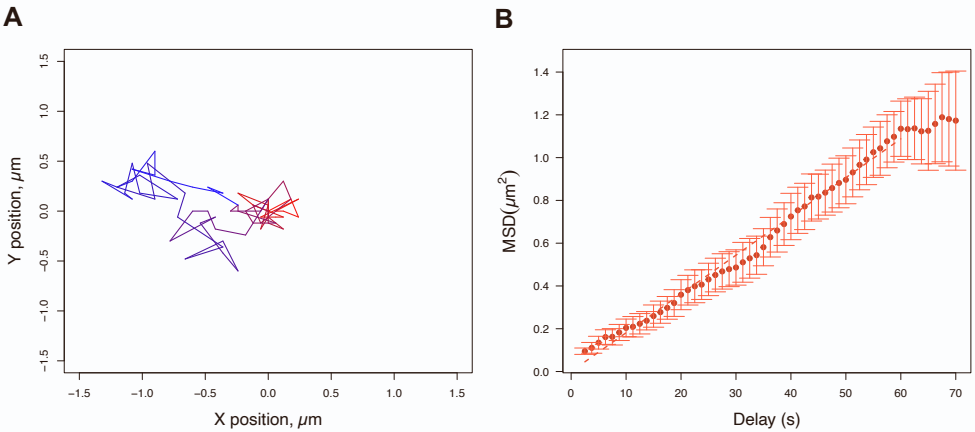

Supplemental Figure 7 Mean Square Displacement analysis of LFY condensates. Related to Figure 2. A, Single trajectory of a representative cytoplasmic LFY condensate in A. *thaliana* over a period of 80 seconds. B, Mean square Displacement (MSD) values of the trajectory in (A), the linear fit to obtain the diffusion coefficient is shown as a dashed line. The error bars represent the standard deviation.

Supplemental Table S1. Primers used in this study, Related to STAR Methods.

Primer names	Aims	Primer sequences (5' → 3')
LFY-attB1	LFY CDS cloning	GGGGACAAGTTTGTACAAAAAAGCAGGCTGGATGGATCCTGAAGGTTTCAC
LFY-attB2	LFY CDS cloning	GGGGACCACTTTGTACAAGAAAGCTGGGTAGAAACGCAAGTCGTCGCCGC
UFO-attB1	UFO CDS cloning	GGGGACAAGTTTGTACAAAAAAGCAGGCTGGATGGATTCAACTGTGTTCAT
UFO-attB2	UFO CDS cloning	GGGGACCACTTTGTACAAGAAAGCTGGGTAACAGACTCCAGGAAATGGAA
ΔFbox -attB1	ΔFbox CDS cloning	GGGGACAAGTTTGTACAAAAAAGCAGGCTGGATGCAACTACTTCCTCTCCGACA
Fbox-attB2	Fbox CDS cloning	GGGGACCACTTTGTACAAGAAAGCTGGGTAAGATATGTCTCGAGGAAGGT
$LFY^{1\text{-}3KR}$-Fw	LFY^{5KR} mutagenesis	GGGACGCAGGTCAAGGAAGGATGAGGAGGCAACAGCAGCAGAGACGG
$LFY^{1\text{-}3KR}$-Rv	LFY^{5KR} mutagenesis	CCGTCTCTGCTGCTGTTGCCTCCTCATCCTTCCTTGACCTGCGTCCC
$LFY^{4\text{-}5KR}$-Fw	LFY^{5KR} mutagenesis	GCAGAGACGGAGAAGGAGACCAATGCTGACGTCAGTGG
$LFY^{4\text{-}5KR}$-Rv	LFY^{5KR} mutagenesis	CCACTGACGTCAGCATTGGTCTCCTTCTCCGTCTCTGC
LFY-Fw	LFY RT-PCR	TCACGCTCTTGATGCTCTCTCC
LFY-Rv	LFY RT-PCR	TCTGTCTCTCTGTCCCCAAACC
UFO-Fw	UFO RT-PCR	ACTTCCTCTCCGACACAAC
UFO-Rv	UFO RT-PCR	ACCCAACTCACTAACCCTCC
EF-1α-Fw	EF-1α RT-PCR	GGTTAAGATGATTCCCACCAAGCC
EF-1α-Rv	EF-1α RT-PCR	GACAACAACAACAGCAACAGTCTG
AP3-Fw	AP3 RT-PCR	GGATAGAGAACCAGACAAAC
AP3-Rv	AP3 RT-PCR	GGTACAGATCTACGATCTCC
Actin2-Fw	Actin2 RT-PCR	GCCCAGAAGTCTTGTTCCAG
Actin2-Rv	Actin2 RT-PCR	TCATACTCGGCCTTGGAGAT
ufo-1-Fw	Genotyping ufo-1	AGATGGTTTACGTGCAAGGC
ufo-1-Rv	Genotyping ufo-1	GTCGTAGGCTTTTGGGAACG